2012

Heme-assisted S-Nitrosation Desensitizes Ferric Soluble Guanylate Cyclase to Nitric Oxide

Nathaniel B. Fernhoff, *University of California, Berkeley*
Emily R. Derbyshire, *University of California, Berkeley*
Eric S. Underbakke, *University of California, Berkeley*
Michael A. Marletta, *The Scripps Research Institute*

THE JOURNAL OF BIOLOGICAL CHEMISTRY VOL. 287, NO. 51, pp. 43053–43062, December 14, 2012
Published in the U.S.A.

Heme-assisted *S*-Nitrosation Desensitizes Ferric Soluble Guanylate Cyclase to Nitric Oxide*[S]

Received for publication, June 20, 2012, and in revised form, October 10, 2012 Published, JBC Papers in Press, October 23, 2012, DOI 10.1074/jbc.M112.393892

Nathaniel B. Fernhoff[‡], Emily R. Derbyshire[‡], Eric S. Underbakke[§¶], and Michael A. Marletta[‡§¶1]

From the Departments of [‡]Molecular and Cell Biology and [§]Chemistry, University of California, Berkeley, California 94720, and the [¶]Department of Chemistry, The Scripps Research Institute, La Jolla, California 92037

Background: Oxidation of the sGC heme iron causes dysfunction in NO/cGMP signal transduction, a key pathway in cardiovascular physiology.
Results: NO treatment of heme-oxidized sGC restores the reduced heme state but concomitantly oxidizes β1Cys-78 and β1Cys-122.
Conclusion: Heme-assisted *S*-nitrosation causes the NO desensitization of ferric sGC.
Significance: This mechanism describes a specific role for protein thiol modification in cardiovascular disease.

Nitric oxide (NO) signaling regulates key processes in cardiovascular physiology, specifically vasodilation, platelet aggregation, and leukocyte rolling. Soluble guanylate cyclase (sGC), the mammalian NO sensor, transduces an NO signal into the classical second messenger cyclic GMP (cGMP). NO binds to the ferrous (Fe^{2+}) oxidation state of the sGC heme cofactor and stimulates formation of cGMP several hundred-fold. Oxidation of the sGC heme to the ferric (Fe^{3+}) state desensitizes the enzyme to NO. The heme-oxidized state of sGC has emerged as a potential therapeutic target in the treatment of cardiovascular disease. Here, we investigate the molecular mechanism of NO desensitization and find that sGC undergoes a reductive nitrosylation reaction that is coupled to the *S*-nitrosation of sGC cysteines. We further characterize the kinetics of NO desensitization and find that heme-assisted nitrosothiol formation of β1Cys-78 and β1Cys-122 causes the NO desensitization of ferric sGC. Finally, we provide evidence that the mechanism of reductive nitrosylation is gated by a conformational change of the protein. These results yield insights into the function and dysfunction of sGC in cardiovascular disease.

Among the diatomic gasses, nitric oxide (NO) is second only to oxygen (O_2) in importance to human health and disease. Although the significance of O_2 in biological systems was first described in 1775 (1), the biological relevance of NO was not demonstrated until 1987 (2). Since then, NO has been shown to effect a myriad of responses in mammalian physiology; it acts as a cytotoxin in the immune system (3), as a neurotransmitter in the nervous system (4, 5), and as a regulator of vasodilation and platelet adhesion in the cardiovascular system (2, 6). The most prominent and best-characterized receptor for NO is soluble guanylate cyclase, a heme-containing enzyme that increases the rate of cGMP synthesis in response to low nanomolar concentrations of NO that bind to the heme cofactor (7). cGMP is a classical second messenger that initiates complex downstream signal transduction cascades. Therefore, the regulation of cGMP levels represents a key checkpoint in cellular signaling. As evidenced in knock-out mice, sGC[2] serves a vital function in mammalian physiology (8).

Cardiovascular disease is often associated with both reduced sGC activity and increased oxidative stress (9, 10), and oxidants have long been known to inhibit sGC function (11, 12). There are three primary routes for oxidants to interfere with NO signaling: the chemical destruction of NO that limits bioavailability (13), the oxidation of sGC thiols that inhibits NO-dependent activation (14–16), and the oxidation of the sGC heme iron that similarly blunts the NO-dependent activation of sGC (17, 18). The role of heme-oxidized sGC in cardiovascular disease is gaining recognition. Indeed, the small molecule therapeutic BAY 58-2667 (Cinaciguat), selectively activates oxidized sGC to ameliorate disease symptoms, as shown in animal models and in human clinical trials (19–21). It has therefore been proposed that the formation of reactive oxygen species causes cardiovascular dysfunction in part through local increases in heme-oxidized sGC (22, 23). Despite the potential importance of heme-oxidized sGC in the pathophysiology of cardiovascular disease, little is known about the molecular mechanism of NO desensitization.

The sGC resting state is characterized by a ferrous (Fe^{2+}) heme iron that binds NO with picomolar affinity to stimulate enzyme activity several hundred-fold (24, 25). However, oxidation of the heme iron to the ferric (Fe^{3+}) state strongly attenuates the enzymatic response to NO (17, 18). Ferric heme generally binds NO with a weaker affinity than ferrous heme (26), but ferric sGC does not simply bind NO in a reversible bimolecular interaction. Ferric sGC undergoes reductive nitrosylation with

* This work was supported, in whole or in part, by National Institutes of Health Grant GM077365. This work was also supported by Bayer Healthcare (Wuppertal, Germany).
[S] This article contains supplemental Methods, Discussion, Table S1, and Figs. S1–S7.
[1] To whom correspondence should be addressed: Dept. of Chemistry, The Scripps Research Institute, 10550 N. Torrey Pines Rd., La Jolla, CA 92037. Tel.: 858-784-8800; Fax: 858-784-8829; E-mail: marletta@scripps.edu.

[2] The abbreviations used are: sGC, soluble guanylate cyclase; α1 and β1, α1 and β1 chain of soluble guanylate cyclase, respectively; DEA/NO, diethylammonium (*Z*)-1-(*N*,*N*-diethylamino)diazen-1-ium-1,2-diolate; ODQ, 1H-(1,2,4)oxadiazolo(4,3-a)quinoxalin-1-one; TCEP, tris(2-carboxyethyl)phosphine; GMPCPP, α,β-methylene guanosine 5′-triphosphate; NEM, *N*-ethylmaleimide.

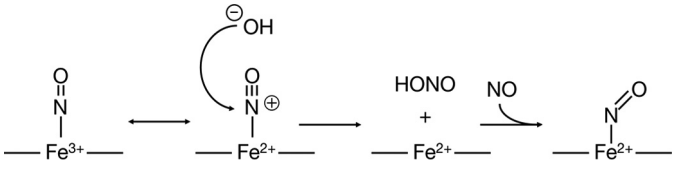

SCHEME 1. **Hydroxide-mediated reductive nitrosylation of ferric heme.**

NO, a reaction reported to occur in other hemoproteins (17, 27). This reaction requires two equivalents of NO. The first NO reduces the ferric iron to generate the ferrous heme. The second equivalent of NO then ligates the heme iron to form a ferrous-nitrosyl complex (Scheme 1). The reductive nitrosylation of ferric sGC presents an apparent incongruity; although the reaction restores the reduced, NO-bound heme state, this enzyme is only partially active. Because the ferrous-nitrosyl complex is regenerated at the heme, the observation of NO desensitization suggests that an additional modification to the protein occurs during the course of the reaction, and this modification prevents the full activation of sGC by NO.

Because the oxidation state of sGC thiols is known to strongly affect cyclase activity, the role of cysteine reactivity in the mechanism of NO desensitization of ferric sGC was investigated. We determined that the reductive nitrosylation of ferric sGC is coupled to heme-assisted nitrosothiol formation and that this *S*-nitrosation of sGC thiols accounts for the inhibition of enzyme activity. Cys-78 and Cys-122 on the β1 subunit were found to be key residues in this process, and a kinetic analysis of reductive nitrosylation further indicated that the overall reaction is gated by a conformational change of the protein. These experiments demonstrate that the heme-assisted *S*-nitrosation of critical β1 cysteine residues causes the NO desensitization of heme-oxidized sGC.

EXPERIMENTAL PROCEDURES

Materials—Rat sGC α1β1, β1(1–194), and β1(1–385) were recombinantly expressed and purified as described previously (28, 29), as was human thioredoxin (30). The NO donor diethylammonium (*Z*)-1-(*N*,*N*-diethylamino)diazen-1-ium-1,2-diolate (DEA/NO) and 1H-(1,2,4)oxadiazolo(4,3-a)quinoxalin-1-one (ODQ) were from Cayman Chemical Co., and stock solutions were made in 10 mM NaOH and DMSO, respectively. GMPCPP was from Jena Biosciences, *N*-ethylmaleimide (NEM) was from Sigma, and NO gas and CO gas were from Praxair. Oligonucleotide primers were obtained from Elim Biopharmaceuticals. Sf9 (*Spodoptera frugiperda*) cells were obtained from the Department of Molecular and Cell Biology Tissue Culture Facility, University of California, Berkeley.

Electronic Absorption Spectroscopy—Absorption spectra were collected on a Cary 3E spectrophotometer (precision ±0.2 nm) with a Neslab RTE-100 temperature controller. Spectra were collected over the range of 350–600 nm at 600 nm/min with a 1-nm data point interval. Anerobic samples were prepared in septum-sealed cuvettes (Starna) by 10 cycles of alternate evacuation and purging with 99.999% argon (Praxair) or in an anaerobic chamber (Coy). Gas-tight syringes were used for all subsequent manipulations.

Preparation of Ferrous and Ferric Complexes and Various Ligand Complexes—Full-length recombinant rat sGC was prepared as described previously (31) except that 1 mM tris(2-carboxyethyl)phosphine (TCEP) was used as a reducing agent instead of dithiothreitol (DTT) during the purification. On the day of the experiment, TCEP was desalted from sGC by four cycles of dilution/concentration using a 10K Ultrafree-0.5 centrifugal filter device (Millipore) with 50 mM Hepes, pH 7.4, 50 mM NaCl anaerobically at 4 °C. Ferric sGC was prepared by incubation with 5 μM ODQ for 1 h at 0 °C and desalted by an additional round of dilution/concentration. Protein concentration and the ferric heme state were verified spectrally using extinction coefficients of 148,000 M^{-1} cm^{-1} for the A_{431} of ferrous sGC (28) and 110,000 M^{-1} cm^{-1} for the A_{392} of ferric sGC (32). β1(1–194) and β1(1–385) were either with treated 1 mM potassium ferricyanide or 1 mM sodium dithionite for 1 h at 4 °C in an anaerobic chamber (Coy) and desalted by 6 cycles of dilution/concentration using a 5K Ultrafree-0.5 centrifugal filter device (Millipore Corp.) with 50 mM Hepes, pH 7.4, 50 mM NaCl at 4 °C. Heme coordination states were assessed spectrally after each manipulation. The CO complex was formed by passing CO gas over the headspace of an anaerobic cuvette of ferrous β1(1–194) at 25 °C, and the NO complex was formed by the subsequent addition of NO gas. The cyanide complex was formed by incubating ferric β1(1–194) with 20 mM NaCN for 20 min at 25 °C.

Preparation of NEM-alkylated Protein—Full-length ferric sGC was either treated with 500 μM NEM (thiol-alkylated) or untreated (native) for 20 min at 37 °C. Identical results were obtained whether or not excess NEM was desalted before reductive nitrosylation assays. β1(1–194) was treated with 10 mM NEM (thiol-alkylated) or untreated (native) for 15 min at 25 °C, and excess NEM was removed by six rounds of dilution/concentration using a 5K Ultrafree-0.5 centrifugal filter device with 50 mM Hepes, pH 7.4, 50 mM NaCl at 4 °C.

Reductive Nitrosylation of Ferric Proteins—1–5 μM thiol-alkylated or native full-length ferric sGC was treated with 50 μM DEA/NO in 50 mM Hepes, pH 7.4, 50 mM NaCl at 37 °C, and the reactions were followed spectrally over time. The kinetic dependence of the reductive nitrosylation rate on the NO concentration was determined by varying the initial concentration of DEA/NO. The difference in absorbance from 392 to 398 nm was plotted *versus* time, and the observed rate was obtained from a single exponential fit of the data. Aerobic nitrosylation reactions of sGC were also performed with similar results. Reductive nitrosylation reactions of β1(1–194) were performed at 25 °C in 50 mM Hepes, pH 7.4, 50 mM NaCl and supplemented with reducing agent where indicated. The amount of DEA/NO for each experiment is specified in the text.

Activity Assays—Duplicate end point assays were performed at 37 °C as described previously (33). 133 nM ferrous or ferric sGC was treated with and without 50 μM DEA/NO in 50 mM Hepes, pH 7.4, 50 mM NaCl. A matched ferric sample was monitored by electronic absorption spectroscopy for 15 min. After the formation of the ferrous-nitrosyl complex was confirmed, the protein was diluted 10-fold into an assay mixture to initiate the enzyme reaction. Assays were initiated with substrate, and the final assay contained 0.2 μg of enzyme in 50 mM

Hepes, pH 7.4, 3 mM $MgCl_2$, 1.5 mM GTP, and, where indicated, 5 mM DTT in a final volume of 100 μl. Reactions were quenched after 2 min by the addition of 400 μl of 125 mM $Zn(CH_3CO_2)_2$ and 500 μl of 125 mM Na_2CO_3. cGMP quantification was carried out using a cGMP enzyme immunoassay kit, Format B (Enzo Life Sciences), per the manufacturer's instructions. All results are given as means ± S.D.

Selective S-Nitrosation of Ferric sGC—Cysteine *S*-nitrosation in the presence and absence of O_2 and NO was determined by the biotin switch method (34) with minor modifications. Aerobically or in an anaerobic chamber, sGC or β1(1–385) was incubated with the indicated amount of DEA/NO for 20 min at 37 °C in 50 mM Hepes, pH 7.4, 50 mM NaCl. Reactions were then quenched aerobically with an equal volume of 250 mM Hepes, pH 7.2, 1 mM EDTA, 0.1 mM neocuproine, 10% SDS, 120 mM NEM. Reactions were transferred to 65 °C for 30 min and vortexed frequently. Samples were then acetone-precipitated, and the protein pellets were subsequently dissolved in 30 μl of 62 mM Hepes, pH 7.2, 0.25 mM EDTA, 0.025 mM neocuproine, 5% SDS, 1 mM maleimide-PEO_2-biotin (Pierce), 10 mM sodium ascorbate, and incubated for 1 h at 25 °C. The reactions were quenched by the addition of SDS-PAGE loading buffer containing 50 mM DTT. The samples were then split and analyzed by both Neutravidin-HRP Western blot and Coomassie Blue staining or anti-sGC Western blot.

Preparation of β1(1–194) Mutants—Mutants of β1(1–194) were generated using the QuikChange XL site-directed mutagenesis kit (Stratagene), according to the manufacturer's instructions. Each substitution was verified by sequencing (University of California, Berkeley, DNA Sequencing Facility), and recombinant β1(1–194) mutants were expressed and purified as described previously (28). The protein purity of all sGC mutants was assessed by SDS-PAGE and was routinely greater than 95%. Protein concentrations were determined using the Bradford microassay (Bio-Rad). Several mutants were isolated without a bound heme cofactor, and these mutants were reconstituted according to a previously published protocol (31).

RESULTS AND DISCUSSION

Ferric sGC Undergoes Reductive Nitrosylation to an NO Desensitized Form of the Ferrous-Nitrosyl Complex—Using electronic absorption spectroscopy and electron paramagnetic resonance (EPR) spectroscopy, Zhao *et al.* (17) previously demonstrated that NO treatment of ferric sGC results in the formation of the ferrous-nitrosyl complex. Although this final ligation state is typically associated with high sGC activity, the activity of NO-stimulated ferric sGC was only a fraction of the activity of NO-stimulated ferrous sGC. Zhao *et al.* (17) speculated that NO treatment of ferric sGC induces only a partial conversion to the ferrous-nitrosyl complex, and the resulting enzyme exists as a heterogeneous mixture of heme states containing only a minor population of the high activity ferrous-nitrosyl species. To investigate this hypothesis, the spectral heterogeneity of NO-stimulated ferric sGC was determined and compared with enzymatic activity.

The extent of conversion and kinetics of reductive nitrosylation of ferric sGC were measured by electronic absorption spectroscopy. Ferric sGC was treated with a 50 μM concentration of the NO donor DEA/NO at 37 °C, and the conversion to the ferrous-nitrosyl complex was monitored over time. The Soret band of ferric sGC (λ_{max} = 392 nm) is readily differentiated from that of the ferrous protein (λ_{max} = 431 nm) (35); after a 30-min incubation with NO, the spectra of NO-treated ferrous and ferric sGC are identical (λ_{max} = 398 nm) (Fig. 1*A*), in agreement with previous EPR characterizations (17, 36). The spectra that result from NO treatment demonstrate the complete conversion of ferric heme to the ferrous-nitrosyl complex. When reductive nitrosylation was monitored over time, the reaction kinetics fit to a single exponential process with a rate of 0.15 ± 0.01 min^{-1} (Fig. 1*B*). Therefore, NO treatment of ferric sGC produces a spectrally homogenous population of ferrous NO-bound sGC, and these observations rule out the hypothesis of partial occupancy to explain the partial stimulation.

Reductive nitrosylation forms a ferrous-nitrosyl complex from ferric sGC that is spectrally identical to the ferrous-nitrosyl complex formed from ferrous sGC. To investigate the consequences of reductive nitrosylation on enzyme kinetics, sGC activity of the ferric-derived ferrous-nitrosyl species was measured. The species was formed (>85% complete) after a 15-min reaction of ferric sGC with NO (Fig. 1*B*). To ensure that excess NO remained in solution, the reaction solution was supplemented with additional NO (0.2 μM DEA/NO) immediately prior to the activity assay. The NO-stimulated activity of the ferric-derived ferrous-nitrosyl complex was only 9% of the NO-stimulated activity of the ferrous-derived ferrous-nitrosyl complex (Fig. 1*C*). This level of desensitization is consistent with previous measurements of ferric sGC activity (17, 18), but here we have combined measurements of enzyme kinetics and spectroscopy to simultaneously interrogate the heme state and active site. These data establish that the fully formed ferrous-nitrosyl complex derived from the reductive nitrosylation of ferric sGC is desensitized to NO relative to the spectrally identical enzyme formed from ferrous sGC.

To further characterize this partially active form of sGC, the sensitivity of reductively nitrosylated sGC to NO was quantified and compared with that of ferrous sGC. Full activation of the ferrous-derived enzyme was observed at 0.2 μM DEA/NO, consistent with the reported EC_{50} of 0.005 μM (7); however, the EC_{50} for reductively nitrosylated sGC is 2.1 ± 0.8 μM (Fig. 1*D*). Moreover, even when maximally stimulated with NO, the reductively nitrosylated sGC is only 30% as active as NO-stimulated ferrous sGC (Fig. 1*D*). Similar results were obtained under both aerobic and anaerobic conditions. These observations suggest a mechanistic basis for the desensitization of ferric sGC to NO. Despite identical heme coordination and redox states, the reductively nitrosylated ferric sGC requires more NO to effect a weaker stimulation than ferrous sGC. The persistence of NO desensitization after the complete conversion to a ferrous-nitrosyl complex suggests that a non-heme modification to sGC has occurred during the process of reductive nitrosylation, and this modification prevents the full NO-activation of the ferric species.

Previous studies of the chemical mechanism of reductive nitrosylation provided a basis for further experiments. The reductive nitrosylation of a ferric hemoprotein was first reported in 1937 (37), when the addition of NO gas to either

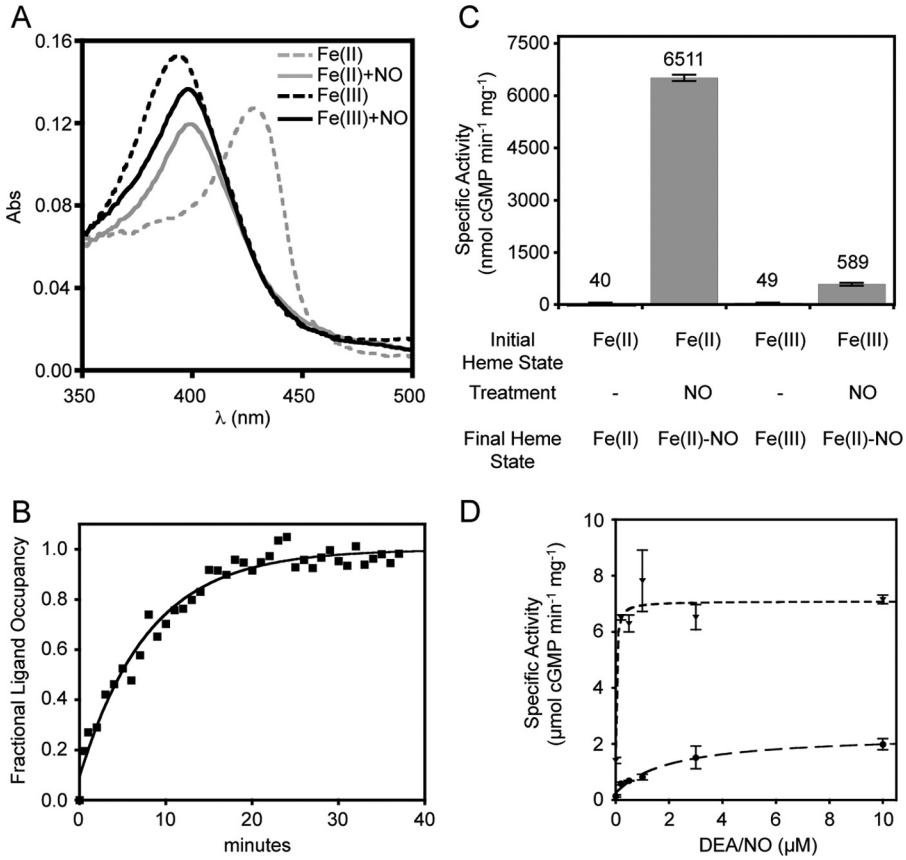

FIGURE 1. **The redox-dependent effects of NO stimulation on sGC at the heme and the active site.** *A*, Fe(II) sGC (800 nM) (heme-reduced) (*gray dotted line*) was treated with 50 μM DEA/NO at 37 °C for 30 min to form the Fe(II)-NO complex (gray *solid line*). Upon identical treatment, Fe(III) sGC (1.5 μM) (heme-oxidized) (*black dotted line*) also converted to a Fe(II)-NO complex (*black solid line*). *B*, Fe(III) sGC was treated with NO as in *A*, and spectra were acquired over time. The fractional ligand occupancy was calculated from the difference in absorbance between the Soret peak of the Fe(II)-NO complex (398 nm) and the Soret peak of Fe(III) sGC (392 nm). *C*, the Fe(II)-NO complex was derived from Fe(II) or Fe(III) sGC by a 15-min treatment with NO. The enzymatic activity of each species was then measured. NO-treated samples were supplemented with 200 nM DEA/NO immediately before initiating the assay to ensure excess NO in solution. *D*, a Fe(II)-NO complex was derived from Fe(II) or Fe(II) sGC as in *C*. The enzymatic activity was measured in response to the amount of the secondary addition of NO. The Fe(II)-derived Fe(II)-NO complex was fully stimulated by 200 nM DEA/NO (*triangles*), whereas the Fe(III)-derived Fe(II)-NO complex exhibited an EC_{50} of 2.1 ± 0.8 μM (*circles*). *Error bars*, S.D.

ferrous or ferric hemoglobin formed identical electronic absorption spectra. Subsequent EPR studies confirmed that the species derived from the NO treatment of ferric hemoglobin was the same ferrous-nitrosyl complex derived from ferrous hemoglobin (38). Reductive nitrosylation proceeds under basic conditions in myoglobin, hemoglobin, neuroglobin, and cytochrome *c* via the nucleophilic attack of a hydroxide ion on the ferric-nitrosyl (Fe^{3+}-NO) complex, shown as an attack on the Fe^{2+}-NO^{+} resonance form in Scheme 1 (27, 39). The hydroxide-mediated reaction liberates an equivalent of nitrite and regenerates the original ferrous heme. Other nucleophiles can substitute for hydroxide, such as glutathione, in the thiol-mediated reductive nitrosylation reaction of cytochrome *c*, which yields the ferrous heme and the corresponding nitrosothiol (40). Similarly in nitrophorin and partially in hemoglobin, a cysteine thiol can act in place of hydroxide, causing reductive nitrosylation at the heme and concomitant *S*-nitrosation of a cysteine residue (41, 42); this particular variation of the reductive nitrosylation reaction has been called heme-assisted *S*-nitrosation.

Activation of sGC by NO is not a simple one-step process. NO first binds to the ferrous heme cofactor of sGC and only partially stimulates the enzyme, but in order to effect full activation, NO must bind to an additional site composed of reduced sGC cysteines (14, 43, 44). Additionally, oxidation of sGC thiols inhibits enzyme activity (14–16). We reasoned that thiol modification during the reductive nitrosylation reaction could similarly manifest as both a decreased sensitivity to NO and an inhibition of maximal stimulation. Therefore, the role of protein thiols in the reductive nitrosylation and subsequent NO desensitization of ferric sGC was investigated.

Thiol Dependence of Reductive Nitrosylation in sGC—Initial experiments to probe the thiol dependence of the reaction utilized the H-NOX (heme-nitric oxide and/or oxygen binding) domain of sGC, which consists of the N-terminal 194 amino acids of the rat β1 subunit. β1(1–194) is purified in high yields and maintains many of the heme ligand binding properties of full-length sGC (45). Similar to full-length sGC, NO induced reductive nitrosylation of ferric β1(1–194). NO treatment caused the spectral transition of the Soret band from 414 to 399 nm, indicative of the conversion from the ferric-aqua state to the ferrous-nitrosyl complex (Fig. 2*A*). To test the role of protein cysteine residues in the reductive nitrosylation reaction, the free thiols of ferric β1(1–194) were alkylated with NEM. After treatment with NO, alkylated β1(1–194) exhibited no change in the Soret maximum (414 nm), indicating that thiol

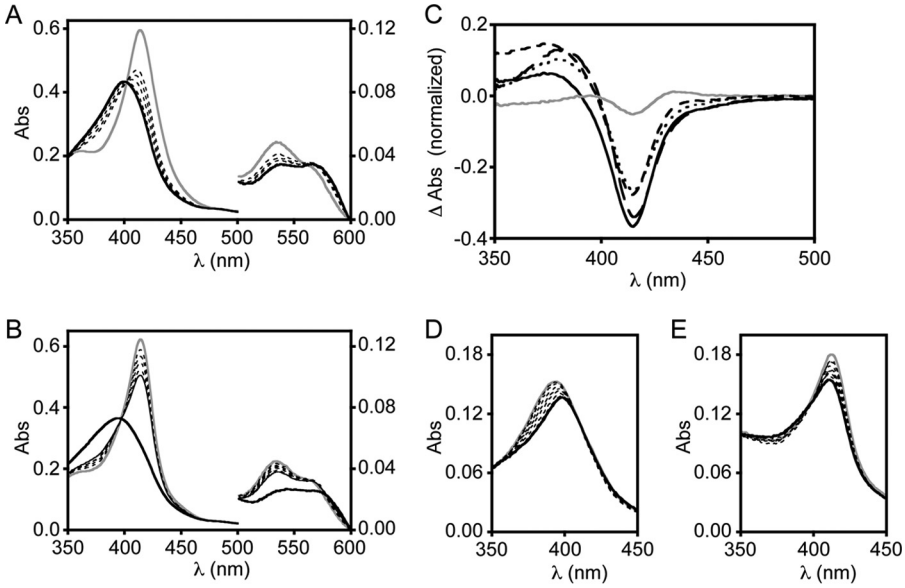

FIGURE 2. **The requirement for a reduced thiol in the reductive nitrosylation of β1(1–194) and full-length sGC.** *A*, native Fe(III) β1(1–194) (*solid gray line*) was treated with 500 μM DEA/NO at 25 °C, and spectra were acquired at 0.5, 1.5, 4, and 8 min (*dotted black lines*) and at 12 min (*solid black line*). The Soret peak transition from 414 to 399 nm reflects the conversion from Fe(III) to the Fe(II)-NO complex. *B*, thiol-alkylated Fe(III) β1(1–194) (*solid gray line*) was treated with NO as in *A*. Spectra were acquired at 0.5, 1.5, 4, and 8 min (*dotted black lines*) and at 12 min (*solid black line*). The unchanged position of the Soret peak at 414 nm represents a stable Fe(III) oxidation state, and the progressive decrease in absorbance indicates heme loss. Co-stimulation of a matched reaction with 1 mM DTT rescued reductive nitrosylation to the thiol-alkylated Fe(III) β1(1–194), restoring the formation of the Fe(II)-NO complex (399 nm) in the same time interval (*heavy solid black line*). *C*, thiol-alkylated Fe(III) β1(1–194) was treated with 250 μM DEA/NO and either 1 mM β-ME (*solid black line*), 1 mM DTT (*long dashed line*), 1 mM GSH (*medium dashed line*), 10 μM thioredoxin (*dotted black line*), or 1 mM TCEP (*solid gray line*) for 15 min at 25 °C. For comparison, data from each reaction are presented as difference spectra from the pretreated spectrum and corrected for progressive heme loss estimated from a matched, untreated control. *D*, full-length Fe(III) sGC (*solid gray line*) was treated with 50 μM DEA/NO at 37 °C, and spectra were acquired at 0.5, 1.5, 3, 6, 8, 12, and 16 min (*dotted black line*) and at 20 min (*solid black line*). As in Fig. 1*A*, the Soret peak shifts from 392 nm (Fe(III)) to 398 nm (Fe(II)-NO). *E*, thiol-alkylated Fe(III) sGC (*solid gray line*) was treated with 50 μM DEA/NO at 37 °C. Spectra were acquired at 0.5, 1.5, 3, 6, 8, 12, and 16 min (*dotted black line*) and at 20 min (*solid black line*). Before the addition of NO, thiol alkylation alone induced a transition of the 392 nm Soret peak to a 413 nm species, both indicative of Fe(III) heme. The Soret peak of thiol-alkylated Fe(III) sGC does not shift appreciably when treated with 50 μM DEA/NO. The decrease in absorbance probably reflects heme loss.

alkylation completely inhibited reductive nitrosylation (Fig. 2*B*).

Like any chemical modification of a protein, NEM treatment risks a broader impact on protein function. For instance, thiol alkylation introduces steric bulk that could nonspecifically prevent ligand access to the heme. To ensure that NEM induced a specific defect in reductive nitrosylation rather than a general inhibition of ligand binding, spectral characterization of the ligand binding properties of the thiol-alkylated β1(1–194) heme iron was carried out. As shown in Table 1, alkylated, ferric β1(1–194) binds cyanide, showing that NEM treatment does not block ligand access to the ferric heme. Additionally, when reduced by dithionite, ferrous thiol-alkylated β1(1–194) bound both CO and NO, which further demonstrates both ligand access to the ferrous heme and the structural integrity of the heme-binding pocket in the NEM-treated protein. Importantly, the observation of NO binding to ferrous thiol-alkylated β1(1–194) confirms that the ferrous-nitrosyl complex can be stably formed. Cumulatively, these data show that thiol alkylation does not block ligand access to the heme iron, but rather it specifically inhibits the process of reductive nitrosylation. In short, a reduced protein thiol drives the chemistry of reductive nitrosylation in sGC.

To explore the potential of exogenous reductants to participate in the reductive nitrosylation of β1(1–194), small molecule thiols were substituted for reduced protein thiols in the reaction. When ferric thiol-alkylated β1(1–194) was treated with 500 μM DEA/NO in the presence of 1 mM DTT, the heme converted from the ferric to the ferrous-nitrosyl complex (Fig. 2*B* and Table 1). Therefore, DTT chemically rescued the defective reductive nitrosylation caused by thiol alkylation. Moreover, many other exogenous thiols were similarly able to rescue the reaction. Treatment with 250 μM DEA/NO and either 1 mM glutathione (GSH), 1 mM β-ME, or 10 μM thioredoxin restored the reductive nitrosylation of thiol-alkylated β1(1–194) (Fig. 2*C*). Interestingly, 1 mM TCEP, a phosphine based reductant, did not restore reductive nitrosylation (Fig. 2*C*), suggesting either that TCEP cannot access the heme or that the phosphine moiety is not a competent nucleophile to participate in the reductive nitrosylation chemistry. These data indicate that the thiol-alkylated protein is structurally competent to undergo reductive nitrosylation but lacks the requisite reduced thiol that would otherwise serve as an intramolecular reductant to drive the reductive nitrosylation reaction.

To assess the thiol dependence of reductive nitrosylation in full-length sGC, ferric sGC was alkylated with NEM. Unexpectedly, thiol alkylation alone induced a spectral shift in the Soret band from 392 to 413 nm (supplemental Fig. S1*A*), suggesting that the 5-coordinate high spin ferric heme had converted to a low spin ferric aqua species similar to the stable ferric state of the β1(1–194) construct. Like ferric β1(1–194), native ferric sGC underwent reductive nitrosylation (Figs. 1*A* and 2*D*); however, thiol-alkylated ferric sGC was not capable of reductive nitrosylation (Fig. 2*E*). When treated with NO, the Soret band of thiol-alkylated ferric sGC decreased in absorbance and slowly transitioned from 413 to 411 nm. This subtle change

TABLE 1

The effect of thiol alkylation by NEM on ligand binding properties of β1(1–194)

Ligand binding was assessed by electronic absorption spectroscopy with 5–10 μM β1(1–194) at 25 °C.

Thiol state[a]	Initial heme state	Ligand	Soret	α/β	Final heme state
			nm	*nm*	
Native	Fe(III)	None[b]	414	565/535	Fe(III)
Native	Fe(III)	NO	399	570/538	Fe(II)-NO
Native	Fe(III)	NO/DTT	399	570/538	Fe(II)-NO
Native	Fe(III)	KCN	418	567/538	Fe(III)-CN
Native	Fe(II)	None[c]	427	560/531	Fe(II)
Native	Fe(II)	NO	398	568/539	Fe(II)-NO
Native	Fe(II)	CO	422	567/540	Fe(II)-CO
Alkylated	Fe(III)	None[b]	414	566/534	Fe(III)
Alkylated	Fe(III)	NO	414	566/534	Fe(III)
Alkylated	Fe(III)	NO/DTT	396	570/539	Fe(II)-NO
Alkylated	Fe(III)	KCN	417	567/538	Fe(III)-CN
Alkylated	Fe(II)	None[c]	427	560/531	Fe(II)
Alkylated	Fe(II)	NO	396	568/539	Fe(II)-NO
Alkylated	Fe(II)	CO	422	567/540	Fe(II)-CO

[a] Protein was either alkylated with 10 mM NEM or untreated for 10 min at 25 °C and then desalted into 50 mM Hepes, pH 7.4, 50 mM NaCl.
[b] Oxidized β1(1–194) initially forms a high spin ferric-unligated species at 392 nm, but it readily converts to a low spin ferric-aqua/hydroxide species at 414 nm (17). This stable low spin species was used in these experiments.
[c] Due to an extremely rapid oxidation of the alkylated β1(1–194), dithionite was in excess to measure the spectral properties of ferrous β1(1–194).

probably reflects heme loss, but a conversion to an alternate ferric conformation is possible. The addition of DTT was similarly able to restore reductive nitrosylation to thiol-alkylated sGC (supplemental Fig. S1*B*). These studies show that a reduced thiol is essential for the reductive nitrosylation of full-length ferric sGC as we observed above for β1(1–194).

Heme-assisted S-Nitrosation Causes NO Desensitization of Ferric sGC—A one-electron reduction of the heme iron is required for reductive nitrosylation (Scheme 1), and our results suggested that an sGC cysteine is the source of this electron. Such a cysteine residue would be concomitantly oxidized during reductive nitrosylation, and we hypothesized that this oxidative protein modification is responsible for the desensitization to NO of ferric sGC. If thiol oxidation inhibits the NO activation of reductively nitrosylated sGC, subsequent thiol reduction should restore NO sensitivity to the enzyme. To test this, the ferrous-nitrosyl complexes derived from either ferrous or ferric sGC were formed as described above, and then each sample was briefly treated with DTT. A 4-min incubation with 5 mM DTT restored the NO-stimulated activity of the ferric-derived sGC to the level of the ferrous-derived sGC (Fig. 3). Therefore, treatment with DTT rescued the NO sensitivity to the ferric-derived form of sGC. The observation that thiol reductants recover enzyme activity suggests that the molecular basis for the NO desensitization of ferric sGC is some form of thiol oxidation.

The reductive nitrosylation of sGC requires a protein thiol to provide one electron for the reaction, and a nitrosothiol is the one-electron oxidation product of nitric oxide and a thiolate anion. Additionally, heme-assisted nitrosothiol formation has been shown to occur concomitantly with the reductive nitrosylation of nitrophorin from *Cimex lectularius* (41) and hemoglobin (42). Therefore, the *S*-nitrosation of sGC cysteines during reductive nitrosylation was investigated.

Initially, the heme domain construct β1(1–385) was used because of the relative stability of the ferrous oxidation state (46). The ferrous and ferric oxidation states were subjected to reductive nitrosylation, and the biotin switch method was used to detect *S*-nitrosation (34). Due to detection limitations of the

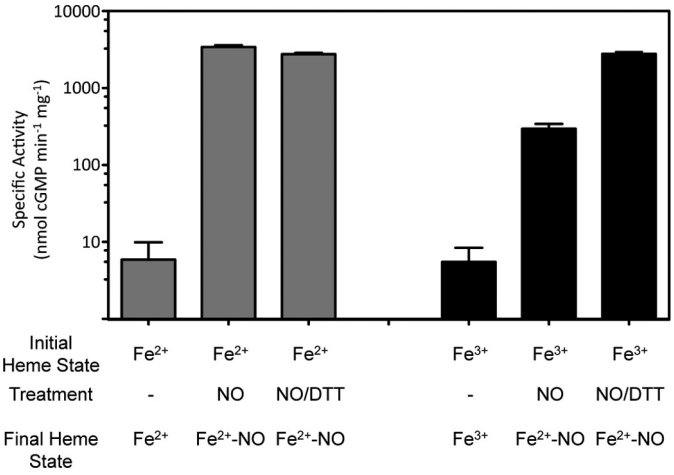

FIGURE 3. **Thiol rescue of reductively nitrosylated sGC activity.** DTT restores the NO-stimulated activity of reductively nitrosylated sGC. Fe(II) or Fe(III) sGC was converted to the Fe(II)-NO complex by treatment with 50 μM DEA/NO for 15 min at 37 °C. DTT (5 mM) was then added to the indicated reactions for 4 min. NO-treated reactions were then supplemented with an additional 50 μM DEA/NO, and the enzyme activity was measured under each condition. *Error bars*, S.D.

biotin switch assay, a higher concentration of DEA/NO was needed to observe nitrosation than to spectrally observe reductive nitrosylation. When the assay was performed aerobically, significant nitrosothiol formation occurred in both oxidation states (supplemental Fig. S2) because NO reacts with O_2 in solution to form higher order nitrogen oxides that result in nonspecific *S*-nitrosation (47). Therefore, ferrous and ferric β1(1–385) were treated anaerobically with NO to eliminate the background of O_2-mediated *S*-nitrosation and to increase the signal for the nitrosothiol formation which is specifically coupled to the reductive nitrosylation of the heme. In the absence of O_2, NO led to *S*-nitrosation of ferric β1(1–385) but not of the ferrous protein (Fig. 4*A*), demonstrating a specific nitrosothiol formation that results from the reductive nitrosylation of the heme iron. To extend these observations to full-length sGC, both ferric and ferrous sGC were anaerobically treated with NO and subjected to the biotin switch assay. Similar to β1(1–385), *S*-nitrosation was observed on the β1 subunit of ferric sGC but

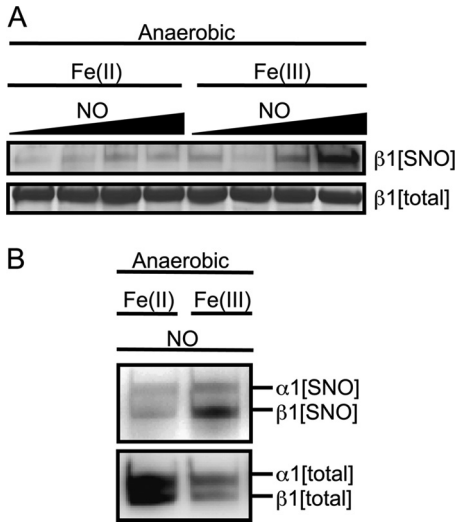

FIGURE 4. **Selective heme-assisted *S*-nitrosation of ferric β1(1–385) and ferric sGC.** *A*, Fe(II) and Fe(III) β1(1–385) were anaerobically treated with 0, 10, 50, or 150 μM DEA/NO (*left to right*) for 20 min at 37 °C and subjected to the biotin switch method (*top*). Coomassie staining of a duplicate gel is shown *below* as a loading control. *B*, Fe(II) and Fe(III) sGC were treated with 150 μM DEA/NO as in *A*, and nitrosothiol formation was observed selectively on the β1 subunit of Fe(III) sGC (*top*). The Western blot was stripped and restained with an anti-sGC antibody as a loading control (*bottom*).

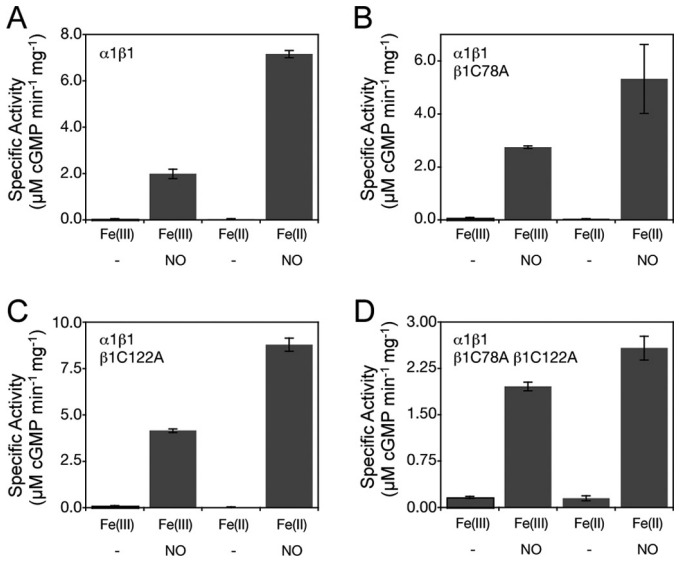

FIGURE 5. **Activity of sGC cysteine mutants.** *A*, Fe(II) or Fe(III) wild-type sGC was converted to the ferrous-nitrosyl complex Fe(II)-NO by 50 μM DEA/NO for 15 min at 37 °C. The enzyme was maximally stimulated with an additional 10 μM DEA/NO, and the activity of each species was measured, as in Fig. 3. The sGC mutants β1C78A (*B*), β1C122A (*C*), and β1C78A/β1C122A (*D*) were subjected to identical treatment as in *A*. *Error bars*, S.D.

not on ferrous sGC (Fig. 4*B*). Densitometry of these bands showed that ferric sGC was labeled >4-fold more than ferrous sGC in the presence of 150 μM DEA/NO. Cumulatively, our results show that after NO stimulation, both ferrous and ferric sGC exhibit identical ferrous-nitrosyl heme coordination states but differ in their final thiol redox states. Specifically, the oxidation of the heme iron is transferred to the oxidation of a protein thiol in the form of a nitrosothiol. Moreover, because thiol reduction can restore NO sensitivity to the reductively nitrosylated sGC, these data suggest that the nitrosothiol formed on sGC cysteines via the heme-assisted mechanism prevents the NO activation of the enzyme.

The Role of β1Cys-78 and β1Cys-122 in the Reductive Nitrosylation and NO Desensitization of sGC—sGC is a heterodimeric protein with a combined molecular mass of 150 kDa and contains 34 cysteine residues; however, the heme domain β1(1–194) contains only 3 cysteine residues distributed in a single 22-kDa domain. Because reductive nitrosylation is thiol-dependent in both sGC and the heme domain, β1(1–194) was used as a model to identify which cysteine is *S*-nitrosated by reductive nitrosylation. Each of the three single point mutants (C78A, C122A, and C174A) and the triple mutant β1(1–194) C78A/C122A/C174A were expressed, purified, and characterized. The ferric form of each mutant was treated with NO at 25 °C, and spectra were acquired over time to monitor reductive nitrosylation. Whereas C122A and C174A exhibited similar spectral conversions as wild-type, C78A and the cysteine-free triple mutant exhibited a spectral transition in the Soret band from 414 to 408 nm (supplemental Fig. S3). This transition to 408 nm was observed even when the C78A mutants were incubated without the addition of NO at 25 °C (supplemental Table S1), indicating that the 408 nm species is probably an alternate form of the ferric heme and not a nitrosyl complex. Functional reductive nitrosylation of the C78A and cysteine-free mutants were restored in the presence of DTT, because both formed the 400 nm Soret band indicative of the five-coordinate ferrous-nitrosyl complex (supplemental Fig. S3). The defective reductive nitrosylation of the C78A mutants suggests that the reduced thiol of Cys-78 is the key cysteine residue that provides the electron to reduce the heme iron in the reaction.

To test the role of β1Cys-78 in the NO desensitization of ferric sGC, the β1C78A mutant in full-length sGC was expressed and purified. The specific activity of this mutant cannot be directly compared with wild-type sGC because activity varies between preparations; therefore, the fold stimulation or percentage change of the basal and NO-stimulated states was evaluated. As described above, ferric wild-type sGC exhibited only ~30% of the maximally NO-stimulated activity of the ferrous enzyme after reductive nitrosylation (Fig. 5*A*). In contrast to predictions based on the β1(1–194) heme domain, the ferric β1C78A sGC underwent functional reductive nitrosylation (supplemental Fig. S4) and exhibited ~50% of the NO-stimulated activity of the ferrous protein (Fig. 5*B*). The modest differences between the C78A mutants and wild-type sGC led us to explore the potential role of other cysteine residues in the NO desensitization of ferric sGC.

Mutation of β1Cys-122 has been reported to protect sGC activity from the oxidative damage of small molecule nitrosothiols, H_2O_2, and aldosterone-induced oxidants (15, 16). To test the role of this residue in the NO desensitization of ferric sGC, the sGC β1C122A mutant was expressed and purified, but again the mutant enzyme underwent reductive nitrosylation and exhibited ~50% of the maximally NO-stimulated activity of its ferrous counterpart (Fig. 5*C*). If *S*-nitrosation of either β1Cys-78 or β1Cys-122 can participate in the NO desensitization of ferric sGC, then significant compensation might occur in either of the single mutants. To test this, the double mutant sGC β1C78A/β1C122A was prepared, and although the

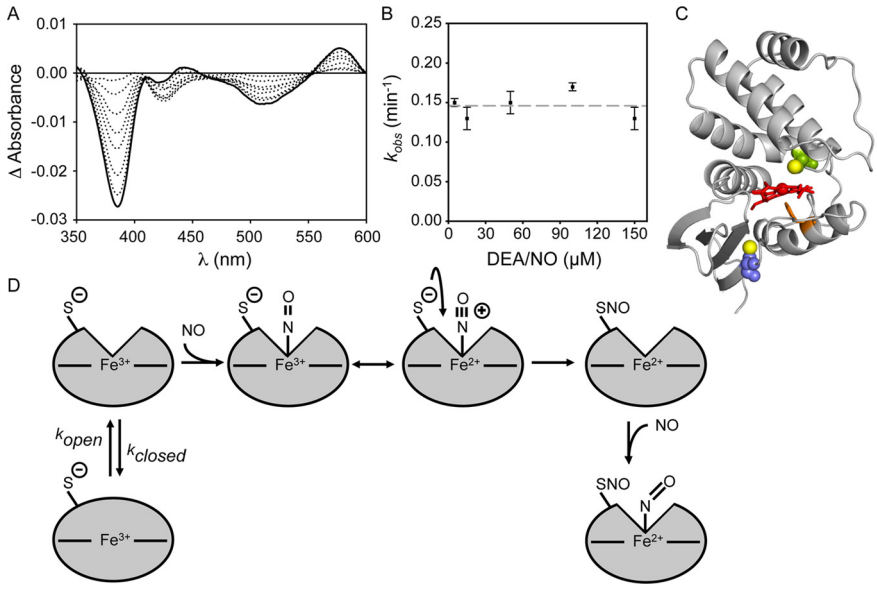

FIGURE 6. **The kinetics and mechanism of reductive nitrosylation in sGC.** *A*, Fe(III) sGC was treated with 50 μM DEA/NO for 15 min at 37 °C, and spectra were recorded at 0.5, 1.5, 3, 6, 8, 12, and 16 min (*dotted black lines*) and at 20 min (*solid black line*). The developing difference spectra exhibit isosbestic points in the transition from the Fe(III) state to the Fe(II)-NO complex without any accumulation of a Fe(III)-NO intermediate. *B*, Fe(III) sGC was treated with the indicated amount of DEA/NO. The rate of reductive nitrosylation was measured as in Fig. 1*B*. A linear fit to the data (*dotted gray line*) verifies the NO independence of the reductive nitrosylation rate. *C*, a homology model of the β1 H-NOX domain shows the relative position of key residues. His-105 (*orange*) ligates the heme iron, Cys-78 (*green*) is located in the distal heme binding pocket, and Cys-122 (*blue*) is ~6.6 Å from the vinyl groups of the heme. *D*, Fe(III) sGC is proposed to equilibrate between open and closed forms. Cys-78 is restricted to an inert position in the closed form, but in the open form, Cys-78 quickly reacts with the NO bound to the Fe(III) heme. This nucleophilic displacement forms a nitrosothiol and a Fe(II) heme, which subsequently binds another equivalent of NO. The final product is an Fe(II)-NO complex that is spectrally identical to the high activity Fe(II)-derived sGC. However, the concomitant *S*-nitrosation modifies the enzyme and prevents stimulation, ultimately causing the NO desensitization of the Fe(III) heme oxidation state. *Error bars*, S.D.

enzyme still underwent reductive nitrosylation, the ferric double mutant displayed ~80% of the maximally NO-stimulated activity of ferrous sGC (Fig. 5*D*). Therefore, the combined mutations of C78A and C122A induced a clear protection of ferric sGC against NO desensitization. The functional reductive nitrosylation of the double mutant does implicate an additional compensation from another sGC thiol in the reduction of the heme iron. However, the resistance against NO desensitization of the ferric double mutant suggests that the *S*-nitrosation of Cys-78 and Cys-122 are the prominent modes of inhibition of heme-oxidized sGC.

Mechanism of Reductive Nitrosylation in sGC—There are two general chemical mechanisms for the thiol-mediated reductive nitrosylation of hemoproteins. The first is an inner sphere electron transfer, where the ferric-nitrosyl complex is subjected to a direct nucleophilic attack from a protein thiol that is located in physical proximity to the heme (supplemental Fig. S5*A*). The second mechanism is an outer sphere electron transfer, where long distance electron transfer from a distant thiol to the ferric-nitrosyl complex causes the transient formation of a ferrous-nitrosyl complex and a thiyl radical. The thiyl radical then reacts quickly with solution NO via radical recombination to yield a nitrosothiol (supplemental Fig. S5*B*). Both mechanisms necessitate the formation of a ferric-nitrosyl complex that precedes the chemistry of the reductive nitrosylation, and detailed studies of the reactions in hemoglobin, myoglobin, and nitrophorin have demonstrated the rapid formation a ferric-nitrosyl complex followed by a slower conversion to the ferrous-nitrosyl complex (27, 39, 41). However, the conversion of ferric sGC to the ferrous-nitrosyl complex does not appear to go through a stable ferric-nitrosyl intermediate. The developing spectra exhibit clear isosbestic points indicative of a two-state reaction with no detectable intermediate (Fig. 6*A*). The only alternative consistent with these mechanisms is that the rate-limiting step of the overall reaction is the formation of the ferric-nitrosyl complex. Therefore, the ferric-nitrosyl intermediate never accumulates because the downstream chemistry of reductive nitrosylation occurs too rapidly. To test if NO association with the ferric heme is the rate-limiting step of the reaction, the kinetics of reductive nitrosylation were determined as a function of [NO]. Because the bimolecular association rate scales linearly with [NO], this scenario necessarily implies that the observed rate of reductive nitrosylation should also scale linearly with [NO]. However, in contradiction to the prediction, the rate of reductive nitrosylation was independent of [NO] between 5 and 150 μM DEA/NO (Fig. 6*B*). Because neither a ferric-nitrosyl intermediate nor a linear dependence on the amount of NO was observed, we conclude that the rate-limiting step of the reaction must occur prior to the association of NO with the enzyme.

The simplest model to reconcile these properties is that ferric sGC equilibrates between an "open" and a "closed" conformation, where the open conformation reacts with NO to undergo reductive nitrosylation but the closed conformation is restricted from undergoing the reaction (Fig. 6*D*). In fact, different sGC conformations of the five-coordinate ferrous-nitrosyl complex have been observed directly by EPR (48), and these multiple conformations regulate both enzyme activity and NO dissociation rates (28, 43, 44). For reductive nitrosylation, we propose that the overall rate-limiting step of the reaction is a relatively slow rate of conformational opening, k_{open}, and then the relatively fast subsequent steps of NO binding and electron

transfer preclude the accumulation of any intermediate or NO dependence. In this proposal, a conformational change of the protein gates the reductive nitrosylation of sGC.

Although there is currently no high resolution structure of sGC, structures of protein homologues to the β1 H-NOX domain have been solved by x-ray crystallography (49–51) and NMR spectroscopy (52). Homology modeling of the β1(1–194) sequence and H-NOX structure from *Thermoanaerobacter tengcongensis* predicts that the thiol side chain of Cys-78 is in the distal heme binding pocket (Fig. 6*C*) and adjacent to the NO ligand. This location suggests that Cys-78 is involved in the heme-assisted *S*-nitrosation via an inner sphere electron transfer (Fig. 6*D*). Cys-122, on the other hand, is predicted to be 6.6 Å from the vinyl group of the heme, and it is therefore more plausible that the heme-assisted *S*-nitrosation of this residue occurs via outer sphere electron (supplemental Fig. S5*B*).

Nucleotide Binding Does Not Inhibit Reductive Nitrosylation or NO Desensitization—Allosteric nucleotide binding strongly affects the NO activation of sGC (43, 44, 53). Preincubation with either GTP or the non-cyclizable GTP analog guanosine-5′-[(α,β) methylene] triphosphate (GMPCPP) sensitizes ferrous sGC to NO. Therefore, we examined the NO desensitization of ferric sGC in the presence of GMPCPP. We found that reductive nitrosylation of ferric sGC proceeds unimpeded when the enzyme is prebound to GMPCPP (supplemental Fig. S6). Furthermore, preincubation with GMPCPP does not sensitize ferric sGC to NO (supplemental Fig. S7). Thus, endogenous nucleotides would not protect ferric sGC from NO desensitization.

CONCLUSION

Upon NO stimulation of ferric sGC, there is a one-electron reduction of the heme iron at the expense of a one-electron oxidation of either Cys-78 or Cys-122. This electron transfer stably transforms the reduced thiol into a nitrosothiol. The *S*-nitrosated sGC that is derived from ferric sGC exhibits two distinct forms of NO desensitization; it requires higher concentrations of NO to effect stimulation, and it has a lower level of activity even when maximally stimulated. Both properties probably contribute to NO desensitization *in vivo*, where NO signaling concentrations are estimated to be in the mid-nanomolar range (54). *In vivo*, we expect the endogenous generation of reactive oxygen species, NO, and thiol reductants to induce heme oxidation, reductive nitrosylation, and thiol-mediated rescue of sGC activity, respectively. The complex interplay of these forces creates a dynamic equilibrium between the NO-sensitive and NO-desensitized sGC states, and the balance has a dramatic impact on human health and disease.

Acknowledgments—We thank Joshua W. Woodward, Brian C. Smith, and Michael B. Winter for numerous insightful discussions.

REFERENCES

1. Priestley, J. (1775) *Experiments and Observations on Different Kinds of Air*, 2nd Ed., J. Johnson, London
2. Palmer, R. M., Ferrige, A. G., and Moncada, S. (1987) Nitric oxide release accounts for the biological activity of endothelium-derived relaxing factor. *Nature* **327,** 524–526
3. Marletta, M. A., Yoon, P. S., Iyengar, R., Leaf, C. D., and Wishnok, J. S. (1988) Macrophage oxidation of L-arginine to nitrite and nitrate. Nitric oxide is an intermediate. *Biochemistry* **27,** 8706–8711
4. Knowles, R. G., Palacios, M., Palmer, R. M., and Moncada, S. (1989) Formation of nitric oxide from L-arginine in the central nervous system. A transduction mechanism for stimulation of the soluble guanylate cyclase. *Proc. Natl. Acad. Sci. U.S.A.* **86,** 5159–5162
5. Bult, H., Boeckxstaens, G. E., Pelckmans, P. A., Jordaens, F. H., Van Maercke, Y. M., and Herman, A. G. (1990) Nitric oxide as an inhibitory non-adrenergic non-cholinergic neurotransmitter. *Nature* **345,** 346–347
6. Radomski, M. W., Palmer, R. M., and Moncada, S. (1987) Endogenous nitric oxide inhibits human platelet adhesion to vascular endothelium. *Lancet* **2,** 1057–1058
7. Gibb, B. J., Wykes, V., and Garthwaite, J. (2003) Properties of NO-activated guanylyl cyclases expressed in cells. *Br. J. Pharmacol.* **139,** 1032–1040
8. Friebe, A., Mergia, E., Dangel, O., Lange, A., and Koesling, D. (2007) Fatal gastrointestinal obstruction and hypertension in mice lacking nitric oxide-sensitive guanylyl cyclase. *Proc. Natl. Acad. Sci. U.S.A.* **104,** 7699–7704
9. Ruetten, H., Zabel, U., Linz, W., and Schmidt, H. H. (1999) Downregulation of soluble guanylyl cyclase in young and aging spontaneously hypertensive rats. *Circ. Res.* **85,** 534–541
10. Harrison, D. G. (1997) Endothelial function and oxidant stress. *Clin. Cardiol.* **20,** II-11–17
11. Brandwein, H. J., Lewicki, J. A., and Murad, F. (1981) Reversible inactivation of guanylate cyclase by mixed disulfide formation. *J. Biol. Chem.* **256,** 2958–2962
12. Braughler, J. M. (1983) Soluble guanylate cyclase activation by nitric oxide and its reversal. Involvement of sulfhydryl group oxidation and reduction. *Biochem. Pharmacol.* **32,** 811–818
13. Kojda, G., and Harrison, D. (1999) Interactions between NO and reactive oxygen species. Pathophysiological importance in atherosclerosis, hypertension, diabetes and heart failure. *Cardiovasc. Res.* **43,** 562–571
14. Fernhoff, N. B., Derbyshire, E. R., and Marletta, M. A. (2009) A nitric oxide/cysteine interaction mediates the activation of soluble guanylate cyclase. *Proc. Natl. Acad. Sci. U.S.A.* **106,** 21602–21607
15. Sayed, N., Baskaran, P., Ma, X., van den Akker, F., and Beuve, A. (2007) Desensitization of soluble guanylyl cyclase, the NO receptor, by *S*-nitrosylation. *Proc. Natl. Acad. Sci. U.S.A.* **104,** 12312–12317
16. Maron, B. A., Zhang, Y. Y., Handy, D. E., Beuve, A., Tang, S. S., Loscalzo, J., and Leopold, J. A. (2009) Aldosterone increases oxidant stress to impair guanylyl cyclase activity by cysteinyl thiol oxidation in vascular smooth muscle cells. *J. Biol. Chem.* **284,** 7665–7672
17. Zhao, Y., Brandish, P. E., DiValentin, M., Schelvis, J. P., Babcock, G. T., and Marletta, M. A. (2000) Inhibition of soluble guanylate cyclase by ODQ. *Biochemistry* **39,** 10848–10854
18. Schrammel, A., Behrends, S., Schmidt, K., Koesling, D., and Mayer, B. (1996) Characterization of 1H-[1,2,4]oxadiazolo[4,3-a]quinoxalin-1-one as a heme-site inhibitor of nitric oxide-sensitive guanylyl cyclase. *Mol. Pharmacol.* **50,** 1–5
19. Stasch, J. P., Schmidt, P. M., Nedvetsky, P. I., Nedvetskaya, T. Y., Arun Kumar, H. S., Meurer, S., Deile, M., Taye, A., Knorr, A., Lapp, H., Müller, H., Turgay, Y., Rothkegel, C., Tersteegen, A., Kemp-Harper, B., Müller-Esterl, W., and Schmidt, H. H. (2006) Targeting the heme-oxidized nitric oxide receptor for selective vasodilatation of diseased blood vessels. *J. Clin. Invest.* **116,** 2552–2561
20. Lapp, H., Mitrovic, V., Franz, N., Heuer, H., Buerke, M., Wolfertz, J., Mueck, W., Unger, S., Wensing, G., and Frey, R. (2009) Cinaciguat (BAY 58-2667) improves cardiopulmonary hemodynamics in patients with acute decompensated heart failure. *Circulation* **119,** 2781–2788
21. Stasch, J. P., Pacher, P., and Evgenov, O. V. (2011) Soluble guanylate cyclase as an emerging therapeutic target in cardiopulmonary disease. *Circulation* **123,** 2263–2273
22. Stasch, J. P., Schmidt, P., Alonso-Alija, C., Apeler, H., Dembowsky, K., Haerter, M., Heil, M., Minuth, T., Perzborn, E., Pleiss, U., Schramm, M., Schröder, W., Schroder, H., Stahl, E., Steinke, W., and Wunder, F. (2002) NO- and haem-independent activation of soluble guanylyl cyclase. Mo-

lecular basis and cardiovascular implications of a new pharmacological principle. *Br. J. Pharmacol.* **136,** 773–783
23. Boerrigter, G., Costello-Boerrigter, L. C., Cataliotti, A., Lapp, H., Stasch, J. P., and Burnett, J. C., Jr. (2007) Targeting heme-oxidized soluble guanylate cyclase in experimental heart failure. *Hypertension* **49,** 1128–1133
24. Stone, J. R., and Marletta, M. A. (1996) Spectral and kinetic studies on the activation of soluble guanylate cyclase by nitric oxide. *Biochemistry* **35,** 1093–1099
25. Zhao, Y., Brandish, P. E., Ballou, D. P., and Marletta, M. A. (1999) A molecular basis for nitric oxide sensing by soluble guanylate cyclase. *Proc. Natl. Acad. Sci. U.S.A.* **96,** 14753–14758
26. Hoshino, M., Laverman, L., and Ford, P. C. (1999) Nitric oxide complexes of metalloporphyrins. An overview of some mechanistic studies. *Coord. Chem. Rev.* **187,** 75–102
27. Hoshino, M., Maeda, M., Konishi, R., Seki, H., and Ford, P. C. (1996) Studies on the reaction mechanism for reductive nitrosylation of ferrihemoproteins in buffer solutions. *J. Am. Chem. Soc.* **118,** 5702–5707
28. Winger, J. A., Derbyshire, E. R., and Marletta, M. A. (2007) Dissociation of nitric oxide from soluble guanylate cyclase and heme-nitric oxide/oxygen binding domain constructs. *J. Biol. Chem.* **282,** 897–907
29. Derbyshire, E. R., and Marletta, M. A. (2007) Butyl isocyanide as a probe of the activation mechanism of soluble guanylate cyclase. Investigating the role of non-heme nitric oxide. *J. Biol. Chem.* **282,** 35741–35748
30. Mitchell, D. A., Morton, S. U., Fernhoff, N. B., and Marletta, M. A. (2007) Thioredoxin is required for *S*-nitrosation of procaspase-3 and the inhibition of apoptosis in Jurkat cells. *Proc. Natl. Acad. Sci. U.S.A.* **104,** 11609–11614
31. Derbyshire, E. R., Deng, S., and Marletta, M. A. (2010) Incorporation of tyrosine and glutamine residues into the soluble guanylate cyclase heme distal pocket alters NO and O_2 binding. *J. Biol. Chem.* **285,** 17471–17478
32. Denninger, J. W., and Marletta, M. A. (1999) Guanylate cyclase and the $^{\bullet}$NO/cGMP signaling pathway. *Biochim. Biophys. Acta* **1411,** 334–350
33. Derbyshire, E. R., Tran, R., Mathies, R. A., and Marletta, M. A. (2005) Characterization of nitrosoalkane binding and activation of soluble guanylate cyclase. *Biochemistry* **44,** 16257–16265
34. Jaffrey, S. R., and Snyder, S. H. (2001) The biotin switch method for the detection of *S*-nitrosylated proteins. *Sci. STKE* **2001,** pl1
35. Stone, J. R., and Marletta, M. A. (1994) Soluble guanylate cyclase from bovine lung. Activation with nitric oxide and carbon monoxide and spectral characterization of the ferrous and ferric states. *Biochemistry* **33,** 5636–5640
36. Stone, J. R., Sands, R. H., Dunham, W. R., and Marletta, M. A. (1995) Electron paramagnetic resonance spectral evidence for the formation of a pentacoordinate nitrosyl-heme complex on soluble guanylate cyclase. *Biochem. Biophys. Res. Commun.* **207,** 572–577
37. Keilin, D., and Hartree, E. F. (1937) Reactions of methaemo-globin and catalase with peroxides and hydrogen donors. *Nature* **139,** 548
38. Sancier, K. M., Freeman, G., and Mills, J. S. (1962) Electron spin resonance of nitric oxide-hemoglobin complexes in solution. *Science* **137,** 752–754
39. Herold, S., Fago, A., Weber, R. E., Dewilde, S., and Moens, L. (2004) Reactivity studies of the Fe(III) and Fe(II)NO forms of human neuroglobin reveal a potential role against oxidative stress. *J. Biol. Chem.* **279,** 22841–22847
40. Basu, S., Keszler, A., Azarova, N. A., Nwanze, N., Perlegas, A., Shiva, S., Broniowska, K. A., Hogg, N., and Kim-Shapiro, D. B. (2010) A novel role for cytochrome *c*. Efficient catalysis of *S*-nitrosothiol formation. *Free Radic. Biol. Med.* **48,** 255–263
41. Weichsel, A., Maes, E. M., Andersen, J. F., Valenzuela, J. G., Shokhireva, T. K., Walker, F. A., and Montfort, W. R. (2005) Heme-assisted *S*-nitrosation of a proximal thiolate in a nitric oxide transport protein. *Proc. Natl. Acad. Sci. U.S.A.* **102,** 594–599
42. Luchsinger, B. P., Rich, E. N., Gow, A. J., Williams, E. M., Stamler, J. S., and Singel, D. J. (2003) Routes to *S*-nitroso-hemoglobin formation with heme redox and preferential reactivity in the β subunits. *Proc. Natl. Acad. Sci. U.S.A.* **100,** 461–466
43. Cary, S. P., Winger, J. A., and Marletta, M. A. (2005) Tonic and acute nitric oxide signaling through soluble guanylate cyclase is mediated by nonheme nitric oxide, ATP, and GTP. *Proc. Natl. Acad. Sci. U.S.A.* **102,** 13064–13069
44. Russwurm, M., and Koesling, D. (2004) NO activation of guanylyl cyclase. *EMBO J.* **23,** 4443–4450
45. Karow, D. S., Pan, D., Davis, J. H., Behrends, S., Mathies, R. A., and Marletta, M. A. (2005) Characterization of functional heme domains from soluble guanylate cyclase. *Biochemistry* **44,** 16266–16274
46. Derbyshire, E. R., Winter, M. B., Ibrahim, M., Deng, S., Spiro, T. G., and Marletta, M. A. (2011) Probing domain interactions in soluble guanylate cyclase. *Biochemistry* **50,** 4281–4290
47. Miersch, S., and Mutus, B. (2005) Protein *S*-nitrosation. Biochemistry and characterization of protein thiol-NO interactions as cellular signals. *Clin. Biochem.* **38,** 777–791
48. Derbyshire, E. R., Gunn, A., Ibrahim, M., Spiro, T. G., Britt, R. D., and Marletta, M. A. (2008) Characterization of two different five-coordinate soluble guanylate cyclase ferrous-nitrosyl complexes. *Biochemistry* **47,** 3892–3899
49. Pellicena, P., Karow, D. S., Boon, E. M., Marletta, M. A., and Kuriyan, J. (2004) Crystal structure of an oxygen-binding heme domain related to soluble guanylate cyclases. *Proc. Natl. Acad. Sci. U.S.A.* **101,** 12854–12859
50. Ma, X., Sayed, N., Beuve, A., and van den Akker, F. (2007) NO and CO differentially activate soluble guanylyl cyclase via a heme pivot-bend mechanism. *EMBO J.* **26,** 578–588
51. Nioche, P., Berka, V., Vipond, J., Minton, N., Tsai, A. L., and Raman, C. S. (2004) Femtomolar sensitivity of a NO sensor from *Clostridium botulinum*. *Science* **306,** 1550–1553
52. Erbil, W. K., Price, M. S., Wemmer, D. E., and Marletta, M. A. (2009) A structural basis for H-NOX signaling in *Shewanella oneidensis* by trapping a histidine kinase inhibitory conformation. *Proc. Natl. Acad. Sci. U.S.A.* **106,** 19753–19760
53. Derbyshire, E. R., Fernhoff, N. B., Deng, S., and Marletta, M. A. (2009) Nucleotide regulation of soluble guanylate cyclase substrate specificity. *Biochemistry* **48,** 7519–7524
54. Tschudi, M. R., Mesaros, S., Lüscher, T. F., and Malinski, T. (1996) Direct *in situ* measurement of nitric oxide in mesenteric resistance arteries. Increased decomposition by superoxide in hypertension. *Hypertension* **27,** 32–35

Heme-assisted *S*-Nitrosation Desensitizes Ferric Soluble Guanylate Cyclase to Nitric Oxide

Nathaniel B. Fernhoff, Emily R. Derbyshire, Eric S. Underbakke and Michael A. Marletta

J. Biol. Chem. 2012, 287:43053-43062.
doi: 10.1074/jbc.M112.393892 originally published online October 23, 2012
